

RESEARCH ARTICLE

Characterization and modulation of the pro-inflammatory effects of immune cells in the canine intervertebral disk

Mary K. Heimann¹  | Kelly Thompson² | Gilian Gunsch³ | Shirley N. Tang¹  | Brett Klamer⁴ | Kara Corps² | Benjamin A. Walter^{1,5}  | Sarah A. Moore² | Devina Purmessur^{1,5} 

¹Department of Biomedical Engineering, The Ohio State University, Columbus, Ohio, USA

²Department of Veterinary Biosciences, The Ohio State University, Columbus, Ohio, USA

³Center for Life Sciences Education, College of Arts and Sciences, The Ohio State University, Ohio, USA

⁴Center for Biostatistics, Department of Biomedical Informatics, College of Medicine, The Ohio State University, Columbus, Ohio, USA

⁵Department of Orthopedics, College of Medicine, The Ohio State University, Ohio, USA

Correspondence

Devina Purmessur, Department of Biomedical Engineering, The Ohio State University, 3016 Fontana Laboratories, 140 W. 19th Avenue, Columbus, OH 43210, USA.

Email: devina.purmessur@osumc.edu; purmessurwalter.1@osu.edu

Funding information

National Institute of Arthritis and Musculoskeletal and Skin Diseases, Grant/Award Number: R21AR077809

Abstract

Background: Intervertebral disk (IVD) degeneration affects both humans and canines and is a major cause of low back pain (LBP). Mast cell (MC) and macrophage (M ϕ) infiltration has been identified in the pathogenesis of IVD degeneration (IVDD) in the human and rodent model but remains understudied in the canine. MC degranulation in the IVD leads to a pro-inflammatory cascade and activates protease activated receptor 2 (PAR2) on IVD cells. The objectives of the present study are to: (1) highlight the pathophysiological changes observed in the degenerate canine IVD, (2) further characterize the inflammatory effect of MCs co-cultured with canine nucleus pulposus (NP) cells, (3) evaluate the effect of construct stiffness on NP and MCs, and (4) identify potential therapeutics to mitigate pathologic changes in the IVD microenvironment.

Methods: Canine IVD tissue was isolated from healthy autopsy research dogs (beagle) and pet dogs undergoing laminectomy for IVD herniation. Morphology, protein content, and inflammatory markers were assessed. NP cells isolated from healthy autopsy (Mongrel hounds) tissue were co-cultured with canine MCs within agarose constructs and treated with cromolyn sodium (CS) and PAR2 antagonist (PAR2A). Gene expression, sulfated glycosaminoglycan content, and stiffness of constructs were assessed.

Results: CD 31+ blood vessels, mast cell tryptase, and macrophage CD 163+ were increased in the degenerate surgical canine tissue compared to healthy autopsy. Pro-inflammatory genes were upregulated when canine NP cells were co-cultured with

This is an open access article under the terms of the [Creative Commons Attribution-NonCommercial-NoDerivs](https://creativecommons.org/licenses/by-nc-nd/4.0/) License, which permits use and distribution in any medium, provided the original work is properly cited, the use is non-commercial and no modifications or adaptations are made.

© 2024 The Authors. *JOR Spine* published by Wiley Periodicals LLC on behalf of Orthopaedic Research Society.

MCs and the stiffer microenvironment enhanced these effects. Treatment with CS and PAR2 inhibitors mediated key pro-inflammatory markers in canine NP cells.

Conclusion: There is increased MC, MØs, and vascular ingrowth in the degenerate canine IVD tissue, similar to observations in the clinical population with IVDD and LBP. MCs co-cultured with canine NP cells drive inflammation, and CS and PAR2A are potential therapeutics that may mitigate the pathophysiology of IVDD in vitro.

KEYWORDS

canine, cromolyn sodium, degeneration, intervertebral disk, low back pain, macrophage, mast cell, protease activated receptor 2

1 | INTRODUCTION

Low back pain (LBP) is a significant global health concern, affecting 577 million people worldwide, and approximately 80% of people will experience LBP at least once in their lifetime.^{1,2} According to The Global Burden of Disease of 2017, LBP is the leading cause of years lived with disability and is a significant contributor to healthcare expenditure and socioeconomic burden in the United States.^{1,3} Additionally, discogenic back pain (DBP) is one of the most common reasons for patients to obtain an opioid prescription and, consequently, a precipitating factor in the opioid crisis.⁴ While many factors such as age, lifestyle, and genetics have been implicated as a driving source for LBP, the exact underlying pathophysiological mechanism remains obscure.⁵ Intervertebral disk (IVD) degeneration (IVDD) has been identified as a major cause of LBP in humans and is a common spinal disorder in canines, affecting on average 2% of pet dogs.^{6,7} While many cases remain asymptomatic in both dogs and humans, herniation is strongly associated with IVDD and clinical signs often results from the encroachment of extruding disk tissue on surrounding neural structures, causing pain and neurological dysfunction.⁸⁻¹⁰

The IVD in both dogs and humans is comprised of three distinct regions: the nucleus pulposus (NP), annulus fibrosus (AF), and cartilaginous end plates (CEPs). The healthy NP is a highly hydrated gelatinous structure with notochordal-derived cells interwoven in a proteoglycan- and collagen-rich matrix, predominantly aggrecan and collagen type II, respectively.^{8,11} The proteoglycan-rich matrix produces swelling pressure inside the NP that is important to withstand compressive forces due to axial loading.¹² The innermost region of the AF encapsulates the NP region and contains a mix of chondrocyte-like cells (CLCs) and fibroblast-like cells (FLCs) in a loose fibrous matrix (mainly collagen type II). The outer AF becomes increasingly more organized with FLCs interspersed on concentric fibrocartilage lamellae (mainly collagen type I).^{8,11} CEPs, comprised of CLCs, anchor the IVD to the adjacent vertebral bodies and act as a semipermeable membrane that is important for regulating nutrient transport to the IVD. The three regions of the IVD form a cohesive functional unit that stabilizes the vertebral column and facilitates movement while also transmitting loads.^{8,11,12}

Pathophysiologic changes in the IVD can be observed as early as 3–4 months in chondrodystrophic dogs (CD) and 10 years of age in

humans.^{9,13,14} During maturation in CD dogs and humans, notochordal cells in the NP are gradually replaced by mature cells that express chondrogenic markers, and proteoglycan content decreases concurrently with an increase in collagen type I.^{8,9,11,15} Degeneration in the AF of both CD dogs and humans is characterized by disruption of the organized lamellae in the outer region, CLC infiltration from the inner AF to the outer AF, and extension of nerve fibers from the outer AF (OAF) to the inner AF and NP regions of the disk.^{8,9,11} In degeneration, the CEPs develop irregular thickness and eventually crack, affecting the selectivity of nutrient transport across the membrane.^{8,9,11}

Current literature has implicated immune system mediators in the pathogenesis of IVD degeneration and DBP in the clinical population and rodent models while the canine model remains understudied.^{13,14} Both mast cells (MCs) and macrophages (MØs) are known to infiltrate the human IVD in degeneration.¹⁶⁻¹⁸ Granulocytic MCs release pro-inflammatory, angiogenic, pain-signaling, and catabolic factors. MCs also stimulate the recruitment of MØs into the IVD, which synthesize additional pro-inflammatory factors associated with IVD herniation matrix remodeling and repair.^{17,18} MØs in the IVD mediate an immune response, influenced by cytokine presence, that can induce or resolve inflammation.¹⁹ While the exact mechanism of herniation resorption is unknown, many studies have attributed this spontaneous phenomenon to the presence of MØs in the IVD.^{19,20} However, the chronic presence of pro-inflammatory cytokines and immune cells in the typically immune-privileged disk initiates and perpetuates the cycle of degeneration by inducing cell death, extracellular matrix (ECM) degradation, and catabolic activity.^{17,18,21,22} Previous work by our group has demonstrated that MC-derived tryptase selectively activates protease activated receptor 2 (PAR2), a G-protein coupled receptor located on a small subpopulation of IVD cells and dorsal root ganglion (DRG) neurons.¹⁸ Persistent activation of PAR2 on IVD cells and DRG neurons can induce sensitization of neuropeptide receptors and functional changes in ion channels located on DRG nociceptors, enhancing hyperalgesia and pain.^{18,23,24}

In addition to immune cell infiltration, angiogenesis in the typically avascular disk has been observed in painful degenerate human IVDs. Angiogenic factors and MC-secreted cytokines foster an environment conducive for pro-angiogenesis in the IVD.^{17,25} Inflammatory mediators have been shown to play a major role in regulating angiogenic factors, considered a precursor for neoinnervation, and pain transmission in the

degenerate disk.²⁶ However, further characterization of the immune system and pro-angiogenic markers in the canine IVD is necessary to understand the canine IVD in both health and disease.

The goals of this study were to: (1) characterize immune cell prevalence and pro-angiogenic pathology in the degenerated canine IVD, (2) characterize canine disk cell-MC interactions, (3) determine the effect of the canine degenerate mechanical environment on disk cell-MC interactions, and (4) identify methods of mitigating pathology in the canine in vitro model (Figure 1).

2 | MATERIALS AND METHODS

Unless otherwise stated, the reagents used in this study are from ThermoFisher Scientific or Sigma Aldrich.

2.1 | Tissue acquisition

Surgical waste tissue (herniated NP ± AF) was collected from 16 client-owned dogs at The Ohio State University Veterinary Medical Center undergoing standard clinical hemilaminectomy without discectomy for the routine care of IVD herniation (IACUC #2019A00000058). Breed information for the dogs can be found in Table S1. Healthy thoracolumbar IVD's were isolated at the time of autopsy from adult beagles ($N = 6$, 1–2 years old) and adult mixed-breed Mongrel hounds from Oak Hill Genetics ($N = 6$, 1–2 years old) that were euthanized in unrelated animal experiments through a tissue sharing program at The Ohio State University Laboratory Animal Resources (IACUC#2018A00000131).

2.2 | Cell isolation and expansion

Spines were collected from the mixed-breed Mongrel hounds within 6 h post-euthanasia. Transverse cuts were made between

each thoracolumbar vertebra to separate individual motion segments. NP cells from each thoracolumbar motion segment were isolated using previously published methods.²⁷ Canine NP cells were expanded in osmotically balanced disk cell complete (ob-DCC) media (400 mOsm/kg, Dulbecco's Modified Eagle Medium (DMEM) 4.5 g/mL glucose, 10% fetal bovine serum (FBS), 1% penicillin streptomycin (P/S), 0.5% amphotericin B, and 0.2% fresh ascorbic acid) through three to four passages. A canine mastocytoma-derived MC line (a gift from Dr. Joelle Fenger, DVM OSU Veterinary Clinical Sciences) was expanded in suspension in mast cell media composed of Roswell Park Memorial Institute (RPMI) 1640 Medium, 10% FBS, 0.02 mg/mL L-proline, 1% P/S, 0.5% 100 mM sodium pyruvate, and 0.5% 1 M 4-(2-hydroxyethyl)-1-piperazineethanesulfonic acid (HEPES). Both MCs and NP cells were cultured in standard normoxia conditions (5% CO₂, 37°C) and fed every 2–3 days until 80% confluent.

2.3 | Seeding NP cells and MCs in 3D agarose

Canine NP cells (P3 or P4) were washed with sterile 1× phosphate buffer saline (PBS), trypsinized, and seeded with a final concentration of 4×10^6 cells/mL in ob-DCC media. Canine MCs were seeded with a final concentration of 5×10^5 cells/mL.¹⁸ Two percent or 8% biological grade 3D Agarose gel (SeaPlaque™ Agarose, catalog #: 50101) was heated and cooled to 50°C. Canine NP cells and MCs were seeded separately (NP only and MC only) or together (NP + MC) in a 1:1 ratio of cell suspension to agarose for a final concentration of either 1% or 4% agarose-cell solution mixture. The agarose-cell solution mixture was homogenized, deposited into a silicone mold, and left to cure for 10 min at room temperature. Cylinders (4 mm thick × 8Ø) of agarose-cell constructs were created using an 8 mm diameter biopsy punch and placed in a 24-well plate with 2 mL of ob-DCC media. Well plates were incubated in standard normoxia conditions (5% CO₂, 37°C) and the media was changed every 2–3 days (see Figure 1).

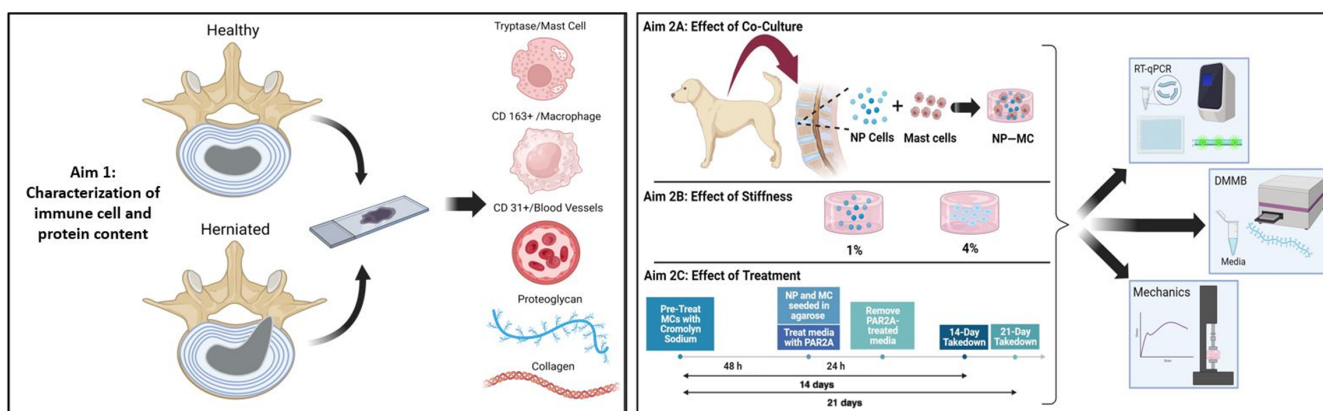


FIGURE 1 Schematic of research design Aims 1 and 2A–C. Figures created using BioRender.com. DMMB, dimethylmethylene blue; MC, mast cell; NP, nucleus pulposus; RT-qPCR, real-time quantitative polymerase chain reaction.

2.4 | PAR2 antagonist and cromolyn sodium

In addition to no treatment controls, canine MCs were pre-treated with 25 μ M of cromolyn sodium (CS; Cayman Chemical 21 379), a mast cell stabilizer, 48 h prior to seeding with canine NP cells in 3D agarose gel (NP + MC + CS) as described above. To assess the anti-inflammatory effects of PAR2A (Tocris Bioscience™ 47-51/1) on co-culture conditions, 100 nM of PAR2A in ob-DCC media was added to NP + MC constructs (NP + MC + P) for 48 h before removing and replacing with fresh ob-DCC media. Both treatments were performed alone (NP + MC + CS and NP + MC + P) or in combination (NP + MC + CS + P). Table 1 provides a full list of the co-culture groups and Table 2 outlines the experimental groups and their respective controls.

2.5 | Downstream assessments

2.5.1 | Proteoglycan/glycosaminoglycan content

Regular ob-DCC media was removed from each well 48 h prior to the 14- or 21-day timepoint and replaced with FBS-free DCC media. At 14 or 21 days, FBS-free DCC media was collected from each well and stored at -80°C . A colorimetric dimethylmethylene blue assay was used to quantify sulfated glycosaminoglycan (sGAG) content in the media using chondroitin sulfate as the standard curve as described previously.²⁸

TABLE 1 Culture groups.

Culture	
NP	NP cells only
MC	MCs only
NP + MC	NP cells co-cultured with MCs
NP + MC + CS	Cromolyn sodium precultured MCs co-cultured with NP cells
NP + MC + P	NP and MCs co-cultured and treated with PAR2A for 48 h
NP + MC + CS + P	Cromolyn sodium precultured MCs co-cultured with NP cells and treated with PAR2A for 48 h

Abbreviations: CS, cromolyn sodium; MC, mast cell; NP, nucleus pulposus; PAR2A, antagonist protease activated receptor 2.

TABLE 2 Experimental controls and comparisons.

	Controls	Comparisons
Effect of co-culture	NP, MC	NP + MC
Effect of stiffness	1%	4%
Effect of treatment	NP + MC	NP + MC + CS NP + MC + P NP + MC + CS + P

Abbreviations: CS, cromolyn sodium; MC, mast cell; NP, nucleus pulposus; PAR2A, antagonist protease activated receptor 2.

2.5.2 | Mechanical testing

After media collection, the dynamic mechanical properties of the hydrogels were assessed. Hydrogels were washed and transferred to the mechanical testing machine (Instron ElectroPuls E3000 LT) and loaded in unconfined compression with an impermeable platen. The mechanical test consisted of initially compressing to 10% strain at a rate of 1%/s. After which, 20 cycles of sinusoidal axial compression with an amplitude of $\pm 2\%$ (i.e., 10%–12%) were applied at 0.1 Hz. The dynamic modulus for each hydrogel was calculated using MATLAB.

2.5.3 | Real-time quantitative polymerase chain reaction

Constructs were assessed for gene expression using previously published methods.²⁷ TaqMan primers utilized are described in Table 3. Gene expression data was normalized to the 18S reference gene; a historically common gene used in vertebrate studies for real-time quantitative polymerase chain reaction (RT-qPCR).^{29,30} The $1/\Delta\text{Ct}$ values were used to analyze the effect of co-culture, NP + MC (1% and 4%), to NP only and MC only controls. The comparative $2^{-\Delta\Delta\text{Ct}}$ method was used to analyze the gene expression for the effect of stiffness and treatment, where the 1% condition and the NP + MC culture served as the controls, respectively.

2.5.4 | Histology and immunohistochemistry

Thoracolumbar NP surgical tissue and individual IVD's isolated from healthy beagles were fixed in 10% neutral buffered formalin (NBF), processed in paraffin, and sectioned on slides for histological

TABLE 3 Taqman gene primers.

Primer	TaqMan assay ID
18S	4333760F
Tryptase	Cf02654863_m1
TAC1	Cf02656283_m1
MMP13	Cf02741638_m1
PAR2	Cf03811559_m1
Toll-like Receptor 4 (TLR4)	Cf02622203_g1
IL-6	Cf02624153_m1
Vascular Endothelial Growth Factor alpha (VEGF α)	Cf02623449_m1
KIT Ligand/Stem Cell Factor (KITLG/SCF)	Cf02625672_m1
Tumor Necrosis Factor alpha (TNF α)	Cf02628236_m1
Interleukin-1 Beta (IL1-B)	Cf02671950_m1
Brachyury (T)	Cf02624791_m1
Nerve Growth Factor (NGF)	Cf02625041_s1

Abbreviation: PAR2, protease activated receptor 2.

assessment. Beagle autopsy and surgical canine tissue sections were stained with hematoxylin and eosin (H&E) and Picrosirius Red and Alcian Blue (PR/AB). Using previously published methods, H&E was used to visualize structural changes at the cellular and tissue level, and PR/AB was used to qualitatively assess collagen and GAG content.^{17,31} Slides were imaged at 10× and 40× magnifications using a Nikon TiE Inverted Microscope.

Immunohistochemistry (IHC) staining was performed on surgical and beagle autopsy samples to determine protein expression for endothelial/blood vessel marker CD 31 (1:100, Abcam ab28364), macrophage marker CD 163 (1:25, Trans Genic Incorporated KT013), and mast cell marker Tryptase (1:100, Santa Cruz Biotechnology sc-59 587). Tissue slides were deparaffinized and rehydrated prior to antigen retrieval via treatment with a Target Retrieval Solution (citrate pH 6.0) for 25 min. The slides for Tryptase did not undergo antigen retrieval. Next, endogenous peroxidase activity was blocked (3% H₂O₂ in MeOH) and serum-free protein block (Agilent, #X0909) was used to reduce non-specific staining. Slides were incubated with the primary antibody in background reducing antibody diluent (DAKO S3022) for 2.5 h for Tryptase, and 30 min for CD 31 and CD 163. The primary antibody was omitted for negative controls performed on the tissue. The slides were then incubated with the biotinylated secondary antibody (1:200, VectorLabs) for 30 min. Finally, the slides were incubated in horseradish peroxidase streptavidin, followed by incubation with 3,3-diaminobenzidine for 2 min (VectorLabs, SK-4100). Gills No. 2 Hematoxylin (Electron Microscopy Sciences 26 030-20) was used as a counterstain, and slides were dehydrated and mounted with coverslips. Slides were imaged at 20× magnification using a Nikon TiE Inverted Microscope. Depending on the tissue size and cell content, between 4 and 10 representative images were taken for each stained slide.¹⁸ Canine lymph tissue was used as positive control tissue for CD 31 and CD 163, and mast cell tumor tissue was used as a positive control for Tryptase. Positive control tissue was imaged at 10× magnification.

The slides were blinded and randomized prior to quantification. The total number of cells and positive-stained cells or blood vessels per tissue region were counted from each image and tissue area was calculated using the microscopes manual tool. The counts from each image were then combined to get a total number for each sample. Percent positivity per tissue area (+ cells/mm²) was calculated for the cells in the NP tissue (surgical and autopsy), cells present in the granulated tissue, and blood vessels for the surgical CD 31 slides (see Figure 1).

2.6 | Statistical analysis

A Mann-Whitney test was used to compare CD 31 percent positivity and the number of blood vessels in surgical and autopsy tissue (Aim 1). A Kruskal-Wallis's test was conducted to compare percent positivity of CD 163 and Tryptase in surgical NP, surgical granulated NP tissue, and autopsy (Aim 1). Linear mixed-effect models with canine-level random intercepts were used to compare NP + MC to

NP and MC controls (Aim 2) and treated co-cultures (NP + MC + CS, NP + MC + P, and NP + MC + CS + P) to NP + MC (Aims 3 and 4) controls for mechanical testing, GAG, and RT-qPCR data. Each model included fixed effects for day of measurement, co-culture, and gel. GAG expressions were log transformed for analysis. The Benjamini-Hochberg procedure was used to calculate false discovery rate (FDR)-adjusted *p*-values among comparisons made within Aims 2–4. An alpha level of 0.05 was chosen for statistical significance. Analyses were conducted using R version 4.1.3 and the lme4 package (version 1.1-28).³²

3 | RESULTS

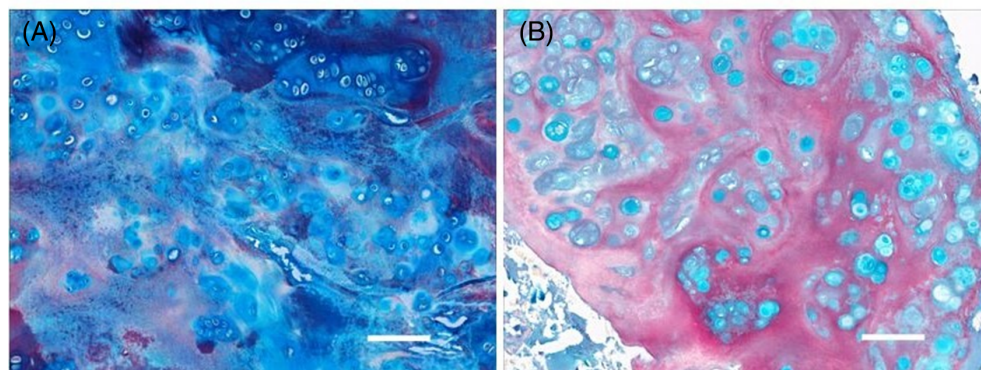
3.1 | Histology and IHC

Picrosirius/alcian blue (PS/AB) staining on NP cells, their surrounding pericellular matrices and ECM in healthy autopsy samples stained predominantly for proteoglycans with a minimal presence of collagen (Figure 2A). Degenerate surgical NP tissue was positive for proteoglycan content while most of the ECM was high in collagen content (Figure 2B). H&E analysis in NP tissue from autopsy samples remained largely intact and NP cells existed in larger clusters compared to surgical samples (Figure 2C). Surgical samples showed NP tissue surrounded by granulation tissue containing FLCs and rays of erythrocytes, consistent with the appearance of blood vessels. NP cells were grouped in small clusters dispersed throughout the ECM (Figure 2D). Granulation tissue, blood vessel structures, and CD 31 positive cells were significantly increased in surgical samples compared to autopsy (Figure 3A–D). Tryptase expression was significantly upregulated in the granulated regions of the NP surgical tissue compared to non-granulated NP surgical tissue and the NP region of healthy autopsy samples (Figure 4A–D). CD 163 was significantly higher in both the NP and granulated regions of surgical samples compared to autopsy (Figure 5A–D).

3.2 | Effect of co-culture

TAC1, IL1 β , and PAR2 were not detected in the majority of samples. IL-6 expression was significantly upregulated in 1% NP + MC co-culture compared to MC control at both the 14- and 21-day timepoints ($p = 0.01$ and $p = 0.03$, respectively). VEGF α was significantly increased in the 1% NP + MC co-culture compared to the MC control at 14 days and the NP control at 21 days ($p = 0.02$ and $p = 0.005$, respectively) (Figure 6A). For the 4% NP + MC co-culture, VEGF α expression at Day 14 and TNF α expression at Day 21 was significantly upregulated compared to the NP control ($p = 0.01$ and $p = 0.01$, respectively) (Figure 6B). While not statistically significant, NP + MC co-cultures contained less sGAG content ($-2.15 \mu\text{g/mL}$) than the NP only control but more sGAG compared to the MC only control ($+0.14 \mu\text{g/mL}$) at both timepoints (Figure S1A). Mechanical testing demonstrated that the dynamic modulus of the NP + MC

Alcian blue/Picrosirius



H&E

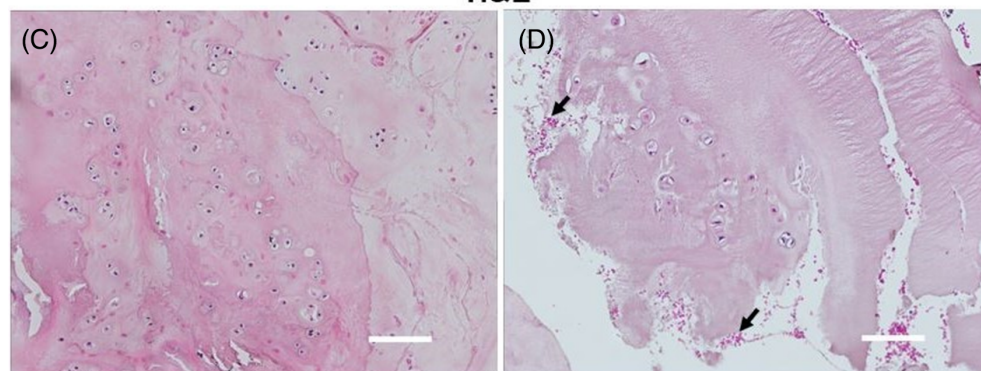


FIGURE 2 Representative images for PS/AB staining in (A) healthy autopsy canine nucleus pulposus (NP) tissue, and (B) degenerate surgical canine NP tissue. Representative hematoxylin and eosin (H&E) images of (C) healthy autopsy canine NP tissue, and (D) degenerate surgical NP tissue with presence of erythrocytes (arrows) in peripheral granulated region. Magnification is 40 \times . Scale bars are 100 μ M.

co-culture group was significantly increased compared to the MC control ($p = 0.003$), averaged across agarose mixture and time. No significant differences were observed between the NP + MC co-culture and NP only control (Figure S2).

3.3 | Effect of stiffness

For the NP control, significant upregulation of NGF on Day 14 and KITLG on Day 21 was observed in the 4% stiffness compared to the 1% ($p = 0.02$ and $p = 0.03$, respectively) (Figure 7A). In the MC control at 14 days, KITLG and TNF α were highly expressed in the 4% stiffness compared to the healthy 1% ($p = 0.04$ and $p = 0.02$, respectively). VEGF α , IL6, and TNF α were significantly upregulated in the stiffer 4% MC control compared to the 1% at Day 21 ($p = 0.047$, $p = 0.02$, $p < 0.001$, respectively) (Figure 7B). The 4% NP + MC co-culture demonstrated an increase in IL-6, VEGF α , and TNF α expression at 21 days compared to the 1%, but this was not statistically significant at 14 days ($p = 0.003$, $p = 0.02$, and $p = 0.001$, respectively) (Figure 7C). For NP + MC + P, IL-6, and TNF α were significantly upregulated in the stiffer 4% environment compared to 1% at 21 days ($p = 0.008$ and $p = 0.005$, respectively) (Figure 7D). While not statistically significant, TNF α expression increased in the 4% stiffness NP + MC + CS + P group compared to the 1% at 21 days ($p = 0.0631$) (Figure 7D). The 4% stiffer environment had overall decreased sGAG ($-0.66 \mu\text{g}/\text{mL}$) compared to the 1% condition, but this was not statistically significant. As anticipated, the overall

dynamic modulus for the 4% groups significantly increased compared to the 1% condition ($p < 0.001$).

3.4 | Effect of pharmacologic treatment

TNF α gene expression was significantly downregulated in the 4% NP + MC + CS and NP + MC + CS + P treatment groups compared to the 4% NP + MC co-culture at 14 days ($p = 0.04$ and $p = 0.01$, respectively). The 4% NP + MC + CS + P condition also significantly decreased TNF α compared to the 4% NP + MC + P group at 14 days ($p = 0.02$) (Figure 8). At 21 days, TNF α was significantly downregulated in the 4% NP + MC + CS treatment group compared to both the 4% NP + MC co-culture and NP + MC + P treatment group ($p = 0.01$ for both). The NP + MC + CS + P treatment sGAG content significantly increased ($+3.13 \mu\text{g}/\text{mL}$) compared to NP + MC + CS treatment ($p = 0.045$) (Figure S1B). No statistically significant differences were observed in the dynamic modulus between the treatment groups (Figure S2).

4 | DISCUSSION

IVD degeneration is a multifactorial process involving changes in ECM, cellularity, inflammation, immune cell infiltration, angiogenesis, and neoinnervation. This complex amalgamation of factors can lead to structure and functional failure of the IVD and DBP.^{17,33} The overall goal of this study was to further characterize the role of immune cells

CD 31

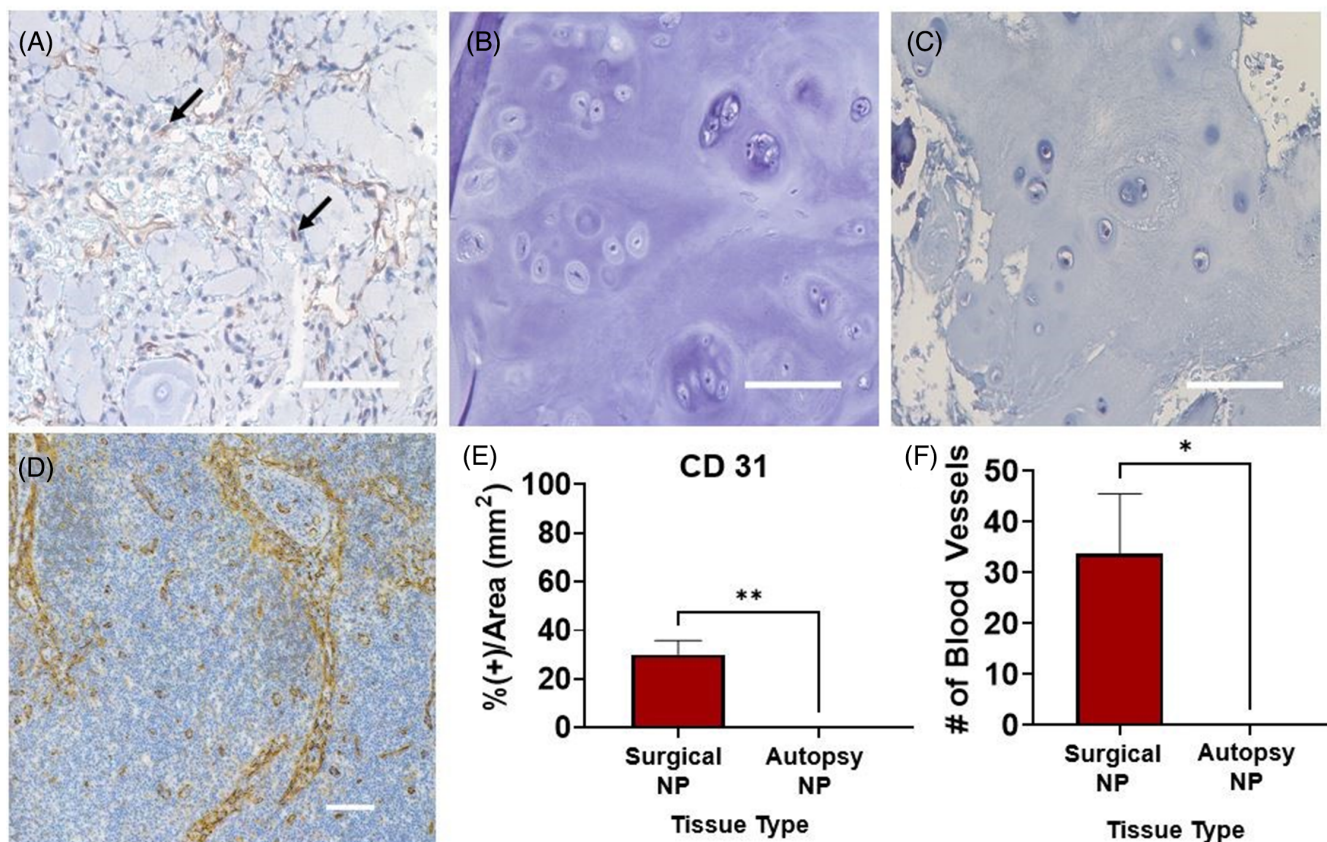


FIGURE 3 (A) Positive CD 31 expression (arrows) in granulated surgical nucleus pulposus (NP). (B) No CD 31 present in autopsy canine NP tissue. (C) Negative control on surgical NP tissue (20 \times magnification). (D) CD 31 staining on positive control lymph tissue (10 \times magnification). (E) Quantification of blood vessel invasion. (F) Quantification of CD 31 percent positivity in degenerate surgical (N = 16) and healthy autopsy (N = 6) canine NP tissue. Scale bars are 100 μ M. **p* value <0.05, ***p* value <0.005. All error bars indicate standard error mean. Statistics = Mann-Whitney test.

in canine IVD degeneration; an understudied yet clinically relevant translational model for IVD degeneration and DBP.¹³ Granulation tissue, a distinct pathologic characteristic in human patients with DBP,³⁴ was present in the canine surgical tissue and absent in the healthy autopsy samples. Granulation tissue is vascularized tissue that forms due to chronic inflammation and plays an important role in wound healing. Typically, M ϕ s and fibroblasts are present, and capillaries in the tissue give a granular appearance.³⁵ We demonstrated an increase in CD 31, Tryptase, and CD 163 positive cells in degenerate canine surgical granulated tissue compared to healthy autopsy tissue, indicating increased MC and M ϕ infiltration and vascular ingrowth, respectively. While CD 163 positivity indicates that M ϕ s are present in the canine NP tissue, these results alone do not indicate whether the M ϕ s are in a pro-inflammatory (M1) or an anti-inflammatory (M2) state.³⁶ In the human IVD, Nakazawa et al. found increased expression of several macrophage markers, including CD 163, in degenerate disks with significant accumulation in granulated tissue of IVDs and our previous work has shown a 53.3% increase in tryptase in the NP of painful surgical human IVDs compared to healthy autopsy controls.^{16,17} In addition, blood vessels are native to the OAF and

CEPs in the healthy human IVD, but extension into other regions may occur as the disk undergoes degenerative changes.³⁷ A study performed by Lama et al. concluded that blood vessel and nerve ingrowth in the clinical population is largely consolidated to the physically disrupted and low-proteoglycan content areas of the disk.³⁷ These findings in humans are consistent with our findings in the canine model of IVDD. Histological evaluation of degenerate human IVD's is marked by a decrease in proteoglycan content with a concurrent increase in collagen content within the NP region of the disk. Similarly, proteoglycan content was largely conserved in the healthy canine NP tissue while the surgical canine NP tissue transitioned to a matrix dominated by collagen. The similar pathological changes observed between dogs and humans further support the canine as a translational model for IVD degeneration and LBP.^{11,13}

In addition to characterizing the presence of immune cells and vascularization within healthy and degenerate canine IVDs, this study sought to further characterize the role of MCs in the pathogenesis of IVD degeneration in the canine model. MCs have been identified in many painful pathological conditions including post-fracture nociception, cancer, and post-operative pain.³⁸ MCs are ubiquitously present

Tryptase

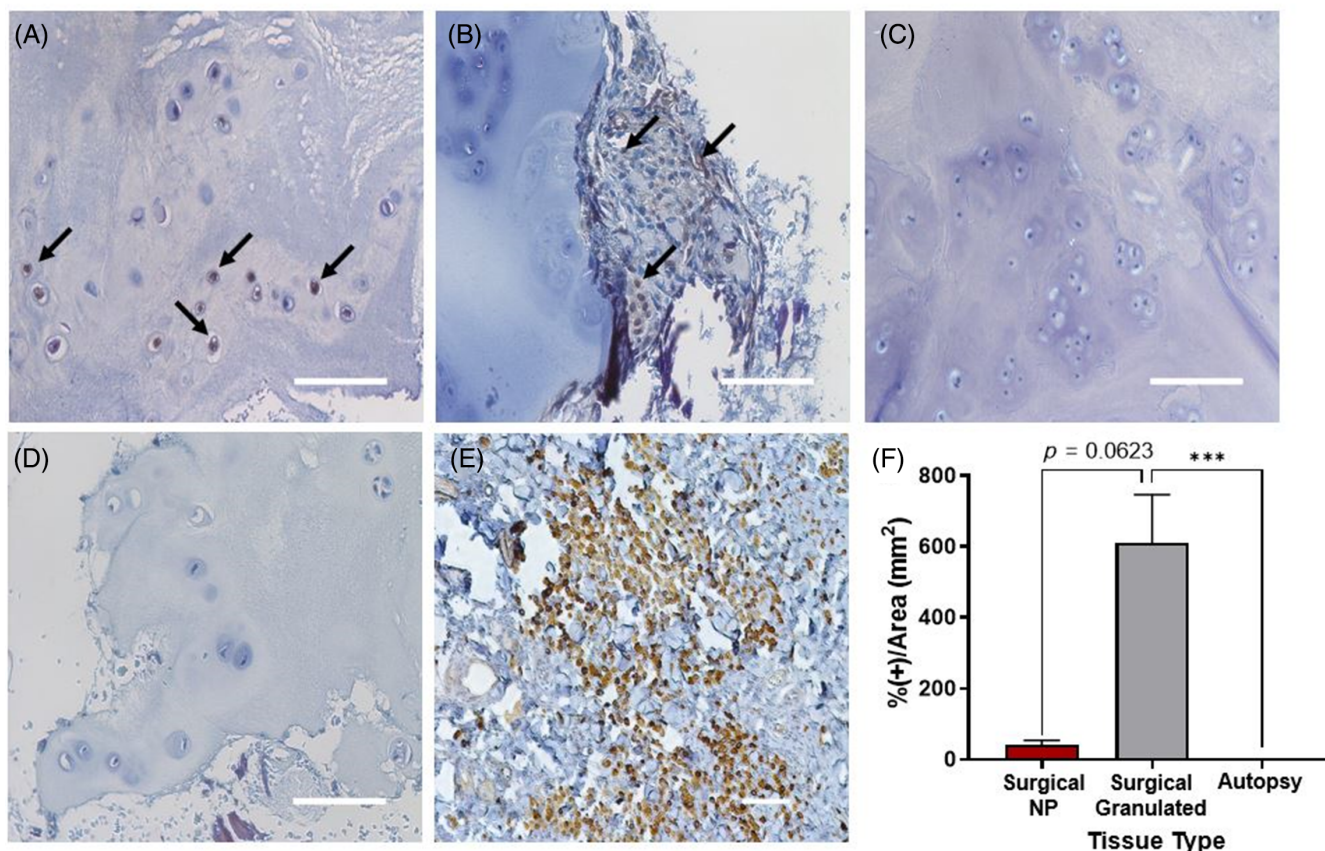


FIGURE 4 (A) Tryptase expression in surgical non-granulated, (B) surgical granulated, and (C) autopsy canine nucleus pulposus (NP) tissue. (D) Negative control for tryptase on surgical canine NP tissue (20× magnification). (E) Tryptase staining on positive control mast cell tumor tissue (10× magnification). (F) Percent positivity in surgical NP ($N = 16$), surgical granulated ($N = 16$), and autopsy ($N = 6$) NP canine tissue normalized to total tissue area. Scale bars are 100 μm . *** p value < 0.0005 . All error bars indicate standard error mean. Statistics = Kruskal-Wallis's test.

in connective tissue and mediate the maintenance of physiological functions, including angiogenesis and homeostasis through degranulation.³⁹ Dysregulation of MC activation has been linked to sustained inflammation and catabolic imbalance and is a significant contributor to the pathophysiological changes observed in the degenerate human IVD.^{17,18,40} Previous work by our group evaluated the effect of MC conditioned media on bovine IVD cells and observed an increase in gene expression of pro-inflammatory and angiogenic factors including, IL6, ADAMTS5, and CCL2/MCP-1.¹⁷ In the present study, canine MCs and NP cells were directly co-cultured in agarose to recapitulate MC invasion in the native microenvironment. Agarose hydrogels have been used in a variety of applications in drug delivery, tissue engineering, and diagnosing of disease. The stiffness properties of agarose support cellular function and activity and are tunable to mimic the environment of the tissue of interest.⁴¹ In humans and dogs, the healthy NP has a high-water content, and this is essential to maintain intradiscal pressure. Loss of proteoglycan in the NP during degeneration leads to lower water content and a stiffer environment.^{8,11} Canine NP and MCs were cultured in 1% or 4% agarose mimicking a softer or stiffer microenvironment representative of the healthy and degenerate states, respectively. Direct co-culture of MCs with NP

cells led to an increase in inflammatory and pro-angiogenic mediators, and these effects were maintained in a stiffer microenvironment which was sustained at 14 and 21 days (Figure 7C).⁴²

Treating the MCs with CS prior to culturing with NP cells led to a decrease in key inflammatory mediators, including $\text{TNF}\alpha$, $\text{VEGF}\alpha$, and KITLG , and some of these effects were observed at both the 14- and 21-day timepoints (Figure 8). CS is a clinically available therapeutic drug approved for use in a variety of different applications in which MCs are important mediators, including asthma, rhinitis, conjunctivitis, and mastocytosis. While the exact mechanism of action of CS is not fully understood, it is hypothesized to stabilize the MC membrane and inhibit the release of granules thereby attenuating the subsequent inflammatory cascade precipitated by MC degranulation.^{42,43} Interestingly, treatment of co-cultures with PAR2A alone did not mitigate the inflammatory response of co-culturing canine MC with NP cells (Figure 8). Previous work by our group evaluated the effects of PAR2A supplemented media on cadaveric human IVD cells in vitro and bovine motion segments ex vivo. In these studies, PAR2A significantly downregulated $\text{VEGF}\alpha$ in the AF region, and enhanced tissue regeneration of the whole bovine IVD. Additionally, PAR2A downregulated an array of chemokine, inflammatory, and neurotrophic genes

CD 163

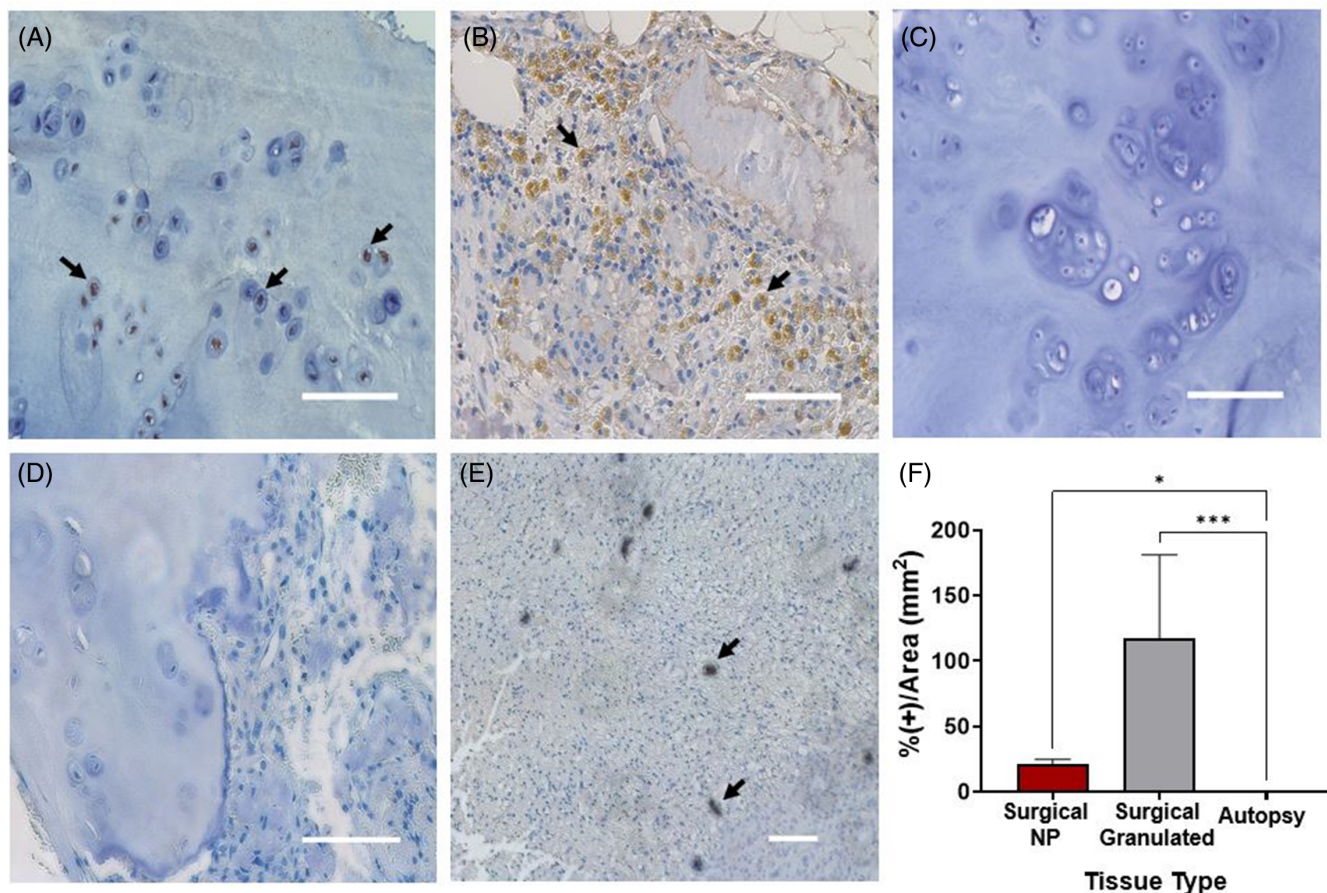
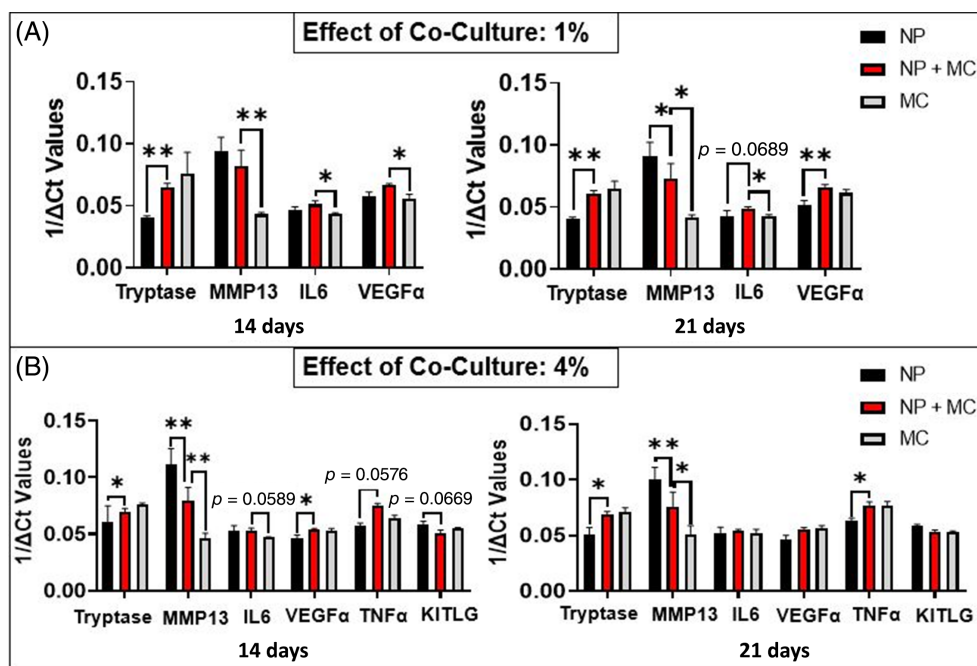


FIGURE 5 (A) CD 163 expression in surgical non-granulated, (B) surgical granulated, and (C) autopsy. (D) Negative control for CD 163 on surgical nucleus pulposus (NP) tissue (20× magnification). (E) CD 163 staining on positive control lymph tissue (10× magnification). (F) Percent positivity of CD 163 in surgical NP ($N = 16$), surgical granulated ($N = 16$), and autopsy ($N = 6$) NP canine tissue normalized to total tissue area. Scale bars are 100 μm . * p value < 0.05, *** p value < 0.0005. All error bars indicate standard error mean. Statistics = Kruskal–Wallis's test.

FIGURE 6 (A) Effect of co-culture in 1% stiffness agarose on gene expression at 14 and 21 days ($N = 3-6$). (B) Effect of co-culture in 4% stiffness agarose on gene expression at 14 and 21 days ($N = 3-6$). * p value < 0.05, ** p value < 0.005. All error bars indicate standard error mean. Statistics = linear mixed model with Benjamini–Hochberg. MC, mast cell; NP, nucleus pulposus.



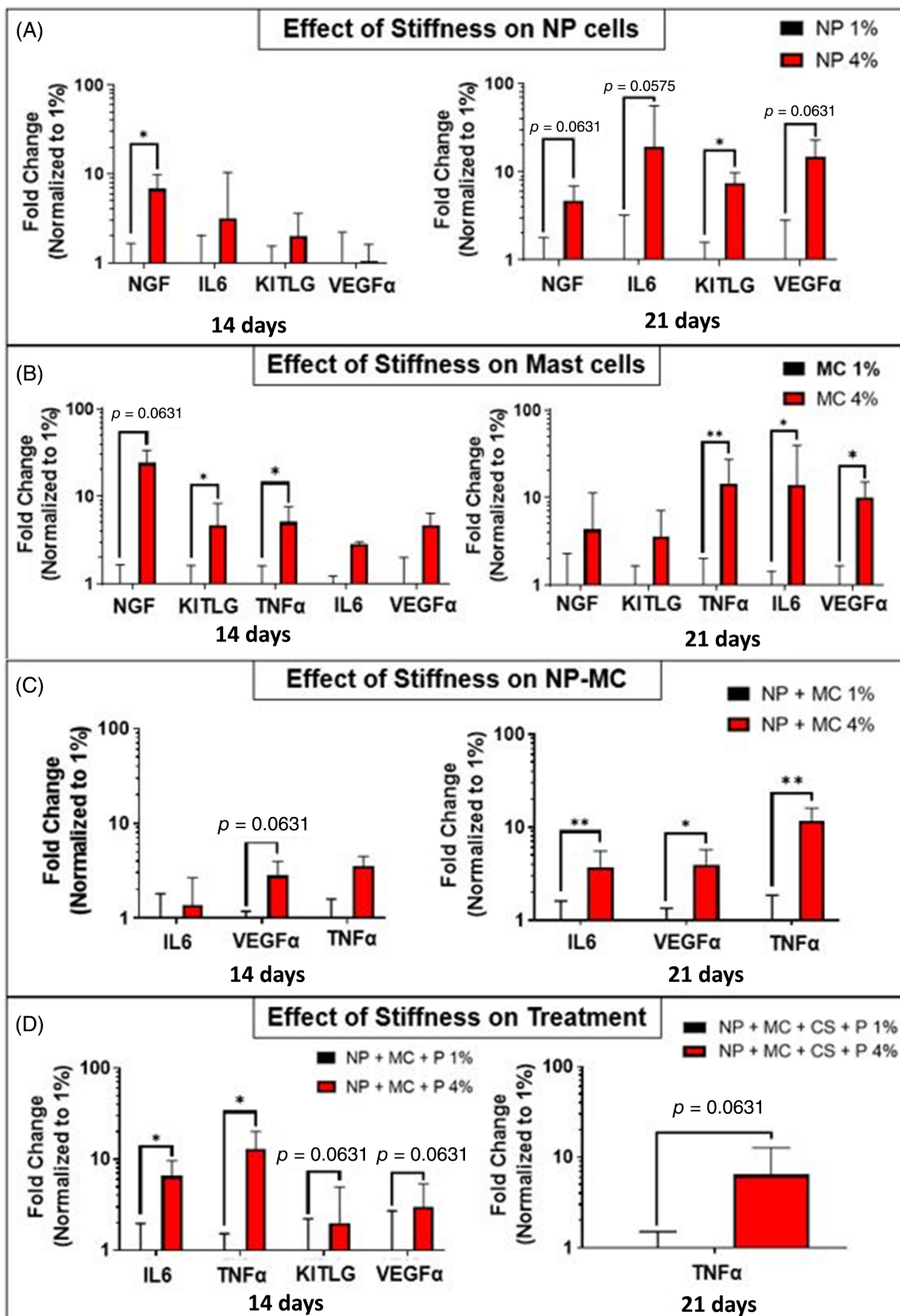


FIGURE 7 (A) Effect of stiffness (1% and 4%) on gene expression of nucleus pulposus (NP) cells at 14 days and 21 days ($N = 3-6$). (B) Effect of stiffness (1% and 4%) on gene expression of mast cells (MCs) at 14 days and 21 days ($N = 3-6$). (C) Effect of stiffness (1% and 4%) on gene expression in the NP + MC co-culture at 14 and 21 days ($N = 3-6$). (D) Effect of stiffness (1% and 4%) on gene expression in treatment groups NP + MC + protease activated receptor 2 antagonist (PAR2A) and NP + MC + cromolyn sodium (CS) + P at 21 days ($N = 3-6$). * p value <0.05, ** p value <0.005. All error bars indicate standard error mean. Statistics = linear mixed model with Benjamini-Hochberg.

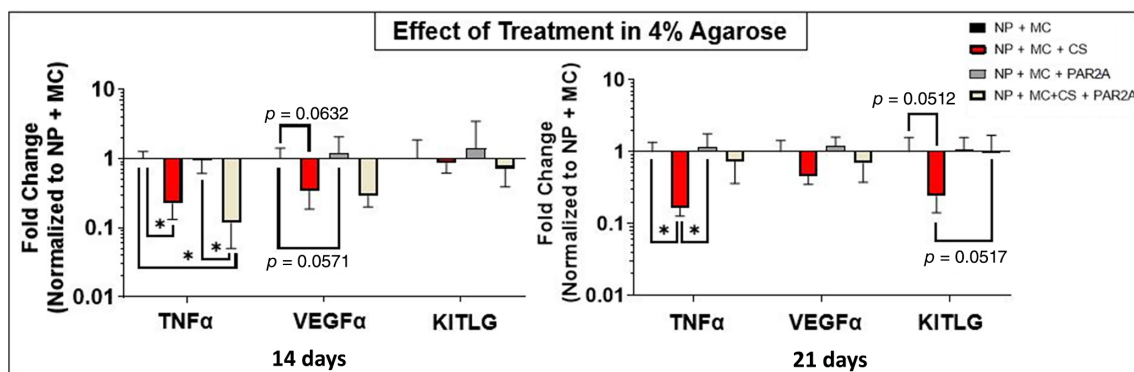


FIGURE 8 Effect of treatment (cromolyn sodium [CS] and/or protease activated receptor 2 antagonist [PAR2A]) on gene expression in the 4% stiffness agarose gel at 14 and 21 days ($N = 3-6$). * p value < 0.05 . All error bars indicate standard error mean. Statistics = linear mixed model with Benjamini-Hochberg. MC, mast cell; NP, nucleus pulposus.

in the human in vitro model with sex differences observed between male and female samples.¹⁸ In the canine model, Kaji et al. and Kim et al. identified a role for PAR2 in canine mammary carcinoma and atopic dermatitis, respectively.^{44,45} However, outside of the present study, little research has explored PAR2 effects on the inflammatory response of canine IVD cells. An inability to account for sex differences due to our sample size or dose of PAR2A chosen may explain why we did not see an effect of PAR2A on the canine immune modulatory pathway. Further characterization of PAR2A and CS is needed to determine whether they are an effective immuno-modulatory therapeutic for the canine model of IVDD and LBP.

While the results provide an understanding of the vascularization and immune infiltration in canine health and disease, and the effect of MCs cultured with NP cells in a 3D environment, there are some limitations in this study. The degenerate canine NP tissue used in the histological and IHC assessments was tissue obtained during a standard surgical procedure for herniation, and it is possible that AF tissue could have been isolated along with the NP tissue. Additionally, surgical tissue isolated from three of the dogs is of unknown breeds. For the co-culture study, NP tissue from mixed-breed Mongrel hounds was used to isolate NP cells, and it is unknown whether these dogs are CD or non-CD. Another potential limitation for the co-culture study is the culturing conditions used for the canine NP and MCs. These cells were cultured in standard normoxia (5% CO₂, 37°C), but hypoxic conditions have been shown to better recapitulate the IVD environment in vivo and differences therefore could impact outcomes; this would be a recommendation for future studies building on this work.⁴⁶ In the current study, there were differences in the total cell densities within the co-culture (NP + MC) and control gels (NP only and MC only). To account for the differences in cell densities between the co-culture and control groups, the ΔCt was used and comparisons were normalized to 18 s values to evaluate the overall change in gene expression between NP + MC and NP or MCs cultured alone rather than direct fold change. However, there were no appropriate methods to account for differences in cell density used for the GAG and mechanics data; therefore, this can be regarded as a potential limitation. Lastly, only GAG released into the media was

measured, but GAG could also be present in the agarose constructs, which was not a measurement of the current study.

Altogether, the results of this study support the canine species as a useful pre-clinical animal model to study IVDD as infiltration of MCs, MØ, and blood vessels is conserved across humans and canine and similar changes in histological pathologies were also observed between the healthy and degenerate IVD of human and canine. The results also support the canine IVD co-culture model as a useful tool for screening immuno-modulatory biologics and investigating mechanisms of IVDD and LBP, but future studies are needed to further evaluate these therapeutics in a clinical setting.

AUTHOR CONTRIBUTIONS

MKH, KT, GG, and SNT performed the experiments and collected data. All authors contributed to the research design, data analysis and interpretation, and drafting and critical review of the manuscript.

ACKNOWLEDGMENTS

Financial support for this project was provided by NIH NIAMS R21AR077809. We thank Kyle Kuchynsky, Connor Gantt, and Lucy Bodine for their technical assistance. Research schematic was created with BioRender. Histology services were provided by the Comparative Pathology and Digital Imaging Shared Resource, Department of Veterinary Biosciences and the Comprehensive Cancer Center, The Ohio State University, Columbus, OH. Devina Purmessur is an Editorial Board member of JOR Spine and co-author of this article. They were excluded from editorial decision-making related to the acceptance of this article for publication in the journal.

CONFLICT OF INTEREST STATEMENT

The authors declare no conflicts of interest.

ORCID

Mary K. Heimann <https://orcid.org/0009-0001-9267-375X>

Shirley N. Tang <https://orcid.org/0000-0001-8807-2348>

Benjamin A. Walter <https://orcid.org/0000-0002-0742-5533>

Devina Purmessur <https://orcid.org/0000-0002-7445-1678>

REFERENCES

- Wu A, March L, Zheng X, et al. Global low back pain prevalence and years lived with disability from 1990 to 2017: estimates from the global burden of disease study 2017. *Ann Transl Med.* 2020;8(6):299. doi:10.21037/atm.2020.02.175
- Taylor JL, Regier NG, Li Q, Liu M, Szanton SL, Skolasky RL. The impact of low back pain and vigorous activity on mental and physical health outcomes in older adults with arthritis. *Front Pain Res (Lausanne).* 2022;3:886985. doi:10.3389/fpain.2022.886985
- Dutmer AL, Schiphorst Preuper HR, Soer R, et al. Personal and societal impact of low Back pain: the Groningen spine cohort. *Spine.* 2019;44(24):E1443-E1451. doi:10.1097/BRS.0000000000003174
- Waljee JF, Brummett CM. Opioid prescribing for low back pain: what is the role of payers? *JAMA Netw Open.* 2018;1(2):e180236. doi:10.1001/jamanetworkopen.2018.0236
- Wong AY, Karppinen J, Samartzis D. Low back pain in older adults: risk factors, management options and future directions. *Scoliosis Spinal Disord.* 2017;12(1):14. doi:10.1186/s13013-017-0121-3
- Rusbridge C. Canine chondrodystrophic intervertebral disc disease (Hansen type I disc disease). *BMC Musculoskelet Disord.* 2015;16:S11. doi:10.1186/1471-2474-16-s1-s11
- Moore SA, Early PJ, Hettlich BF. Practice patterns in the management of acute intervertebral disc herniation in dogs. *J Small Anim Pract.* 2016;57(8):409-415. doi:10.1111/jsap.12496
- Urban JP, Roberts S. Degeneration of the intervertebral disc. *Arthritis Res Ther.* 2003;5(120):120-130.
- Smolders LA, Bergknot N, Grinwis GCM, et al. Intervertebral disc degeneration in the dog. Part 2: chondrodystrophic and non-chondrodystrophic breeds. *Vet J.* 2013;195(3):292-299. doi:10.1016/j.tvjl.2012.10.011
- Jeffery ND, Levine JM, Olby NJ, Stein VM. Intervertebral disk degeneration in dogs: consequences, diagnosis, treatment, and future directions. *J Vet Intern Med.* 2013;27(6):1318-1333. doi:10.1111/jvim.12183
- Bergknot N, Smolders LA, Grinwis GCM, et al. Intervertebral disc degeneration in the dog. Part 1: anatomy and physiology of the intervertebral disc and characteristics of intervertebral disc degeneration. *Vet J.* 2013;195(3):282-291. doi:10.1016/j.tvjl.2012.10.024
- Lundon K, Bolton K. Structure and function of the lumbar intervertebral disk in health, aging, and pathologic conditions. *J Orthop Sports Phys Ther.* 2001;31:291-306.
- Thompson K, Moore S, Tang S, Wiet M, Purmessur D. The chondrodystrophic dog: a clinically relevant intermediate-sized animal model for the study of intervertebral disc-associated spinal pain. *JOR Spine.* 2018;1(1):e1011. doi:10.1002/jsp2.1011
- Lyu FJ, Cui H, Pan H, et al. Painful intervertebral disc degeneration and inflammation: from laboratory evidence to clinical interventions. *Bone Res.* 2021;9(1):7. doi:10.1038/s41413-020-00125-x
- Nerurkar NL, Elliott DM, Mauck RL. Mechanical design criteria for intervertebral disc tissue engineering. *J Biomech.* 2010;43(6):1017-1030. doi:10.1016/j.jbiomech.2009.12.001
- Nakazawa KR, Walter BA, Laudier DM, et al. Accumulation and localization of macrophage phenotypes with human intervertebral disc degeneration. *Spine J.* 2018;18(2):343-356. doi:10.1016/j.spinee.2017.09.018
- Wiet MG, Piscioneri A, Khan SN, Ballinger MN, Hoyland JA, Purmessur D. Mast cell-intervertebral disc cell interactions regulate inflammation, catabolism and angiogenesis in discogenic back pain. *Sci Rep.* 2017;7(1):1-14. doi:10.1038/s41598-017-12666-z
- Richards J, Tang S, Gunsch G, et al. Mast cell/proteinase activated receptor 2 (PAR2) mediated interactions in the pathogenesis of discogenic back pain. *Front Cell Neurosci.* 2019;13:294. doi:10.3389/fncel.2019.00294
- Vizcaino Revés N, Mogel HM, Stoffel M, Summerfield A, Forterre F. Polarization of macrophages in epidural inflammation induced by canine intervertebral disc herniation. *Front Vet Sci.* 2020;7:7. doi:10.3389/fvets.2020.00032
- Teplick JG, Haskin ME. Spontaneous regression of herniated nucleus pulposus. *Am J Neuroradiol.* 1985;6(3):331-335. doi:10.1097/md.00000000000014667
- Ye F, Lyu FJ, Wang H, Zheng Z. The involvement of immune system in intervertebral disc herniation and degeneration. *JOR Spine.* 2022;5(1):e1196. doi:10.1002/jsp2.1196
- Le Maitre CL, Pockert A, Buttle DJ, Freemont AJ, Hoyland JA. Matrix synthesis and degradation in human intervertebral disc degeneration. *Biochem Soc Trans.* 2007;35(pt 4):652-655. doi:10.1042/BST0350652
- Bennett DL, Alex Clark XJ, Huang J, Waxman SG, Dib-Hajj SD. The role of voltage-gated sodium channels in pain signaling. *Physiol Rev.* 2019;99(2):1079-1151. doi:10.1152/physrev.00052.2017
- Chen Y, Yang C, Wang ZJ. Proteinase-activated receptor 2 sensitizes transient receptor potential vanilloid 1, transient receptor potential vanilloid 4, and transient receptor potential ankyrin 1 in paclitaxel-induced neuropathic pain. *Neuroscience.* 2011;193:440-451. doi:10.1016/j.neuroscience.2011.06.085
- Ucuzian AA, Gassman AA, East AT, Greisler HP. Molecular mediators of angiogenesis. *J Burn Care Res.* 2010;31(1):158-175. doi:10.1097/BCR.0b013e3181c7ed82
- Binch A LA, Cole AA, Breakwell LM, et al. Expression and regulation of neurotrophic and angiogenic factors during human intervertebral disc degeneration. *Arthritis Res Ther.* 2014;16(5):416. doi:10.1186/s13075-014-0416-1
- Tang S, Richards J, Khan S, et al. Nonviral transfection with Brachyury reprograms human intervertebral disc cells to a pro-anabolic anti-catabolic/inflammatory phenotype: a proof of concept study. *J Orthop Res.* 2019;37(11):2389-2400. doi:10.1002/jor.24408
- Mort JS, Roughley PJ. Measurement of glycosaminoglycan release from cartilage explants. *Methods Mol Med.* 2007;135:201-209. doi:10.1007/978-1-59745-401-8_12
- Chapman JR, Waldenström J. With reference to reference genes: a systematic review of endogenous controls in gene expression studies. *PLoS One.* 2015;10(11):e0141853. doi:10.1371/journal.pone.0141853
- Suzuki T, Higgins PJ, Crawford DR. Control selection for RNA quantification. *Biotechniques.* 2000;29:332-337.
- Cardiff RD, Miller CH, Munn RJ. Manual hematoxylin and eosin staining of mouse tissue sections. *Cold Spring Harb Protoc.* 2014;2014(6):655-658. doi:10.1101/pdb.prot073411
- Bates D, Mächler M, Bolker B, Walker S. Fitting linear mixed-effects models using lme4. *J Stat Softw.* 2015;67(1):1-48. doi:10.18637/jss.v067.i01
- Adams MA, Roughley PJ. What is intervertebral disc degeneration, and what causes it? *Spine.* 2006;31(18):2151-2161.
- Peng B, Hao J, Hou S, et al. Possible pathogenesis of painful intervertebral disc degeneration. *Spine.* 2006;31(5):560-566.
- Jones K. Fibrotic response to biomaterials and all associated sequence of fibrosis. *Host Response to Biomaterials: the Impact of Host Response on Biomaterial Selection.* Elsevier Inc; 2015:189-237. doi:10.1016/B978-0-12-800196-7.00009-8
- Barros MHM, Hauck F, Dreyer JH, Kempkes B, Niedobitek G. Macrophage polarisation: an immunohistochemical approach for identifying M1 and M2 macrophages. *PLoS One.* 2013;8(11):e80908. doi:10.1371/journal.pone.0080908
- Lama P, Le Maitre CL, Harding IJ, Dolan P, Adams MA. Nerves and blood vessels in degenerated intervertebral discs are confined to physically disrupted tissue. *J Anat.* 2018;233(1):86-97. doi:10.1111/joa.12817
- Mai L, Liu Q, Huang F, He H, Fan W. Involvement of mast cells in the pathophysiology of pain. *Front Cell Neurosci.* 2021;15:15. doi:10.3389/fncel.2021.665066

39. Krystel-Whittemore M, Dileepan KN, Wood JG. Mast cell: a multi-functional master cell. *Front Immunol*. 2016;6:620. doi:[10.3389/fimmu.2015.00620](https://doi.org/10.3389/fimmu.2015.00620)
40. Aich A, Afrin LB, Gupta K. Mast cell-mediated mechanisms of nociception. *Int J Mol Sci*. 2015;16(12):29069-29092. doi:[10.3390/ijms161226151](https://doi.org/10.3390/ijms161226151)
41. Salati MA, Khazai J, Tahmuri AM, et al. Agarose-based biomaterials: opportunities and challenges in cartilage tissue engineering. *Polymers*. 2020;12(5):1150. doi:[10.3390/POLYM12051150](https://doi.org/10.3390/POLYM12051150)
42. Storms W, Kaliner MA. Cromolyn sodium: fitting an old friend into current asthma treatment. *J Asthma*. 2005;42(2):79-89. doi:[10.1081/JAS-52017](https://doi.org/10.1081/JAS-52017)
43. Oka T, Kalesnikoff J, Starkl P, Tsai M, Galli SJ. Evidence questioning cromolyns effectiveness and selectivity as a mast cell stabilizer in mice. *Lab Invest*. 2012;92(10):1472-1482. doi:[10.1038/labinvest.2012.116](https://doi.org/10.1038/labinvest.2012.116)
44. Kaji K, Kaji N, Hori M, Sakai K, Yonezawa T, Maeda S. Protease-activated receptor-2 is associated with adverse outcomes in canine mammary carcinoma. *Vet Pathol*. 2021;58(1):53-62. doi:[10.1177/0300985820963087](https://doi.org/10.1177/0300985820963087)
45. Kim HJ, Jeong SK, Hong SJ, Ahrens K, Marsella R. Effects of PAR2 antagonist on inflammatory signals and tight junction expression in protease-activated canine primary epithelial keratinocytes. *Exp Dermatol*. 2017;26(1):86-88. doi:[10.1111/exd.13121](https://doi.org/10.1111/exd.13121)
46. Feng G, Li L, Liu H, et al. Hypoxia differentially regulates human nucleus pulposus and annulus fibrosus cell extracellular matrix production in 3D scaffolds. *Osteoarthr Cartil*. 2013;21(4):582-588. doi:[10.1016/j.joca.2013.01.001](https://doi.org/10.1016/j.joca.2013.01.001)

SUPPORTING INFORMATION

Additional supporting information can be found online in the Supporting Information section at the end of this article.

How to cite this article: Heimann MK, Thompson K, Gunsch G, et al. Characterization and modulation of the pro-inflammatory effects of immune cells in the canine intervertebral disk. *JOR Spine*. 2024;7(2):e1333. doi:[10.1002/jsp2.1333](https://doi.org/10.1002/jsp2.1333)